https://doi.org/10.1016/j.expthermflusci.2020.110064

Nanosecond laser irradiation of soot particles: insights on structure and optical properties

F. Migliorini [a,*], S. De Iuliis [a], R. Dondè [a], M. Commodo [b], P. Minutolo [b], A. D'Anna [c]

[a] *Istituto di Chimica della Materia Condensata e Tecnologie per l'Energia, CNR-ICMATE, Via R. Cozzi 53, 20125 Milano, Italy*

[b] *Istituto di Ricerche sulla Combustione, CNR, P.le Tecchio 80, 80125, Napoli, Italy*

[c] *Università degli Studi di Napoli Federico II, Dipartimento di Ingegneria Chimica, dei Materiali e della Produzione Industriale, P.le V. Tecchio 80, 80125 Napoli, Italy*

* Corresponding author: Francesca Migliorini (francesca.migliorini@cnr.it)

https://doi.org/10.1016/j.expthermflusci.2020.110064

Abstract

In spite of the advances in laser diagnostics in combustion, the effect of rapid laser irradiation on the physical/chemical properties of soot particles is far from being comprehensively understood. Optical properties, particle nanostructure and aggregate size of laser-irradiated soot particles are analyzed in this paper. Carbonaceous particles sampled from nitrogen-quenched diffusion flames of ethylene and methane are irradiated on-line by a 1064-nm short laser pulse. Wavelength-resolved extinction measurements in the visible range are used to follow their transformation by varying the laser energy density. A variation of the extinction coefficient of the irradiated particles compared to the extinction coefficient of the pristine ones is observed, especially for ethylene soot. The particle nanostructures are analyzed by Raman spectroscopy and the effect of laser irradiation on aggregate structure is evaluated by measuring particle size distributions. The results indicate that both soot nanostructure and optical properties are strongly dependent on the laser energy density when irradiated by a laser source. This is significant for ethylene soot, while for methane soot the degree of variation of such properties is less pronounced, at least in the investigated heating conditions.

Keywords

Soot, laser-heating, LII, nanostructure, optical properties, Raman spectroscopy.

https://doi.org/10.1016/j.expthermflusci.2020.110064

1. Introduction

Combustion soot varies in its morphology and chemistry depending on the type of fuel and the combustion conditions. Knowing the physico-chemical properties of soot particles is very important for practical applications as well as for assessing their impact on human health and on the environment [1-2]. Particularly, the optical properties of these particles and aggregates have been widely investigated especially for evaluating soot contribution to radiative forcing and earth albedo and for determining their concentration through optical-based diagnostics [3-5]. Among them, Laser-Induced Incandescence (LII) has been widely used in the last years to evaluate particle volume fraction and primary particle size in flames, at the exhaust of combustion systems and in the environment [5-6]. The technique involves the heating of soot particles to the incandescence temperature, using a high-power, pulsed or continuous wave, laser. Two are the key parameters to take into account when using a laser source for irradiating particles: the laser wavelength and the fluence. Soot particles absorb over a broad wavelength range and the absorption cross-section increases with decreasing wavelengths. The use of visible and near-IR laser beam for particle irradiation leads to an increase in the particle temperature and to the emission of a quasi-blackbody radiation [7]. Laser fluence is known to principally affect the particle temperature which increases with the fluence until it reaches a maximum at the sublimation temperature (about 4000K) [8-9]. The fluence vaporization threshold depends on the excitation wavelength and on the chemical composition of the particles [9]. For laser fluences higher than the vaporization threshold, other phenomena, such as production of gas-phase carbon cluster, reduction in particle size, could occur.

Such intense laser radiation has been proved to significantly modify the particles internal structure [10-11], induce sublimation and loss of material from soot particles and also promote the formation of new particles as a result of a vaporization effect [12].

Many research efforts have been devoted to study the influence of pulsed laser heating on soot optical properties. Back in 1998, Vander Wal et al. [13] first explored such effect in a laminar diffusion flame of ethylene. The results of a double pulse experiment showed that a modest heating by the first laser pulse enhanced the LII signal induced by the second pulse and therefore the absorption and emission characteristics of the particles under investigation. This enhancement was believed to be permanent and due to annealing and graphitization processes. Using fluences higher than 0.2 J/cm^2, an increasing mass loss was visualized by TEM, and a decrease in the second LII signal was observed which was attributed to changes in the soot optical properties. Witze et al. [14] measured extinction and scattering coefficient of 1064-nm laser heated soot particles in a propane diffusion flame performing LII, elastic light scattering

https://doi.org/10.1016/j.expthermflusci.2020.110064

and pulse-integrated extinction measurements simultaneously. The results showed that the extinction coefficient of heated soot increases by about 20% as the fluence increases for values below 0.2 J/cm^2. This effect was attributed to the thermal annealing or to an increase in the temperature-dependent absorptivity. For fluences higher than 0.2 J/cm^2 a substantial mass loss occurred, resulting in a monotonically decrease of the extinction coefficient, in agreement with the observation of Vander Wal et al. [13]. Similar results have been obtained by Michelsen et al. [8]. The absorption and scattering cross section of soot were investigated by coupling LII and time-averaged extinction measurements; an enhancement of the extinction coefficient was initially observed as the 1064-nm laser fluence was increased to about 0.2 J/cm^2. Beyond this fluence threshold, the extinction coefficient decreased presumably due to soot sublimation.

More recently it was also observed that soot particles of different ages behave differently when irradiated by a strong laser pulse. Olofsson et al. [15] studied the fluence threshold of soot sublimation in a premixed/air flame at various heights, corresponding to different ages of soot. It was found that the fluence above which the elastic light scattering signal dropped was higher for the young, less graphitic soot present at low flame heights. This behavior was explained by assuming that young soot particles have a lower soot refractive index absorption function, *E(m)*, compared to the mature soot particles at high flame heights, which are characterized by a more graphitized structure.

Later, Saffaripour et al. [16] extended the investigation to both premixed and diffusion flames. A rapid enhancement of the extinction coefficient during laser heating was observed in both flames, with the premixed one showing the more significant variation. This was attributed to the different ages and temperature/gas composition histories of soot in the two flames. The spectral dependence of the extinction coefficient enhancement was associated to thermal annealing effects. At high laser fluences, the enhancement of the extinction coefficient was followed by a rapid decay attributed to loss of soot material. A secondary rise in extinction coefficient was observed from 50 to 800 ns after the laser pulse, at low wavelengths attributed to the formation of light-absorbing gaseous species from the sublimated soot. These results only partially agree with the data of Thomson et al. [17], who performed similar measurements on soot particles at ambient temperature. Time-resolved attenuation measurements at 405 and 830 nm were performed on cooled soot particles while simultaneously heating the aerosol with a strong 1064-nm laser pulse. From low to moderate laser fluences, a reversible increase of the extinction coefficient at 830 nm was observed. This effect was attributed to a temperature dependence of *E(m)*. At low laser fluence, a small permanent increase of *E(m)* was observed, most likely related to soot graphitization. Extinction measurements at 405 nm showed a

https://doi.org/10.1016/j.expthermflusci.2020.110064

significantly different trend. For the entire fluence range, an initial decline of the extinction coefficient during the laser-heating process is followed by a substantial increase. The authors explained such behaviour by the vaporization of absorbed volatile species, which continued to absorb the 405 nm radiation when desorbed. This effect is predominant on other effects such as thermal annealing or temperature-dependence of $E(m)$ and therefore the initial enhancement of the extinction coefficient, observed at 830 nm, was not detected. The dissimilarities between the works by Saffaripour et al. [16] and Thomson et al. [17] were attributed to a stronger contribution of the gas phase species present in the flame to light attenuation and to the significant difference between the initial temperature of the particles and the temperature of the surrounding gases.

These studies have clearly shown that laser irradiation of soot significantly affects the physical and/or chemical nature of the particles in quite a complex way. Often the result is a change in the absorption, scattering and incandescence properties during laser irradiation although it is not clear whether those changes are permanent, reversible and possibly wavelength-dependent. Moreover, a clear correlation between optical properties, nanostructure and particles morphology is still missing.

It is evident that understanding the physicochemical processes happening during laser irradiation is mandatory for the development and correct application of laser-based diagnostics techniques. On the other hand, the development of a controlled laser irradiation process of soot particles could be exploited for obtaining carbonaceous particles with tailored characteristics, i.e., size, morphology and optical properties. Moreover, Singh et al. [18] recently demonstrated that controlled pulsed laser annealing of soot particles enhances slight differences in nanostructure and chemical composition and can then be used as an analytical tool for soot differentiation by condition/sources.

The aim of the present work is to study the effect of laser irradiation on soot particles in term of optical properties, particles nanostructure as well as aggregate morphology. The experimental conditions are chosen on the basis of previous works, which showed, via LII and TEM investigations, that intense laser pulses produce relevant effects on soot particles. These effects also depend on the fuel type [9-11]. To further investigate how the different nature of the soot affects the laser heating process, in this work wavelength-resolved extinction measurements of non-irradiated and laser-irradiated soot particles were performed. A range of laser fluences up to the sublimation temperature was explored. On-line measurements were carried out on particles sampled in two quenched co-flow diffusion flame of ethylene and methane after the particles have cooled down to the surrounding gas environment. Particle size

https://doi.org/10.1016/j.expthermflusci.2020.110064

distribution of non-irradiated and laser-irradiated soot was also measured to obtain information on aggregates morphology. Finally, Raman spectroscopy was used to emphasize differences in soot nanostructure.

2. Experimental set-up

Measurements were performed on soot particles produced by a custom-made soot generator, consisting of a quenched coflow diffusion flame at atmospheric pressure [9,11]. A metallic ring is placed around the flame at a variable height above the burner nozzle. Inside the ring, eight 1-mm-diameter nozzles point symmetrically towards the vertical axis of the burner. Nitrogen jetting from the nozzles quenches the flame.

In order to generate soot with different characteristics (loading and maturity), three changes in the soot generator operating conditions are possible: the hydrocarbon fuel, the fuel flow rate (visible flame height) and the quenching height. In this paper, two flame configurations were adopted: an ethylene and a methane flame both quenched at 30 mm and having a visible flame height of 65 mm. In this way, soot particles with a different degree of maturity are formed. Details of the flame operating conditions are reported in Table 1.

The quenched flame exhausts were mixed with the coflowing air and then confined in a small cylindrical chimney, see Fig.1. In the case of ethylene, a dilution tunnel flowing air was implemented to reduce the high soot load. At the exit of the tunnel, a stainless steel extracting probe is used to sample the particles, that, at this point, have cooled down to ambient temperature and therefore will be referred to as “cold soot” from now on.

Table 1. Soot generator working conditions.

fuel	Fuel flow rate [l/min]	Air Coflow [l/min]	Visible unquenched flame height [mm]	N_2 [l/min]	Quenching height [mm]
CH_4	0.29	1.63	65	0.28	30
C_2H_4	0.15	1.77	65	0.19	30

Cold soot particles were then sampled into an irradiation cell, which consists of a 18 cm long glass tube equipped with two quartz windows at the tube entrance and exit. Here, the particles were irradiated by the fundamental harmonic of a Nd:YAG laser (Quantel, Big-Sky, CFR 400). The beam diameter (∅ = 5 mm) was equal to the tube inner diameter and had a top-hat intensity profile ensuring that all the soot particles in the tube were uniformly irradiated. The sampling flow rate was adjusted to 1 l/min, thus the particles residence time in the tube

https://doi.org/10.1016/j.expthermflusci.2020.110064

was approximately 0.2 s. Therefore, the laser frequency was set at 5 Hz to ensure that the sampled particles were irradiated only by a single laser pulse. A beam attenuator was placed in front of the tube in order to vary the laser energy density in the range 0 - 0.7 J/cm^2.

The irradiation cell is followed by a second tube, where on-line extinction measurements were performed. This quartz tube was 25.5 cm long and had an inner diameter of 5 mm. An intense diffuse Halogen lamp (400 W) was used as light source and the transmitted signal was collected on an optical quartz fiber (Oriel, 3 mm bundle diameter) coupled with a Czerny-Turner spectrograph (Shamrock 303i) connected to an ICCD camera (iStar 334T, Andor Technology). A long pass filter at 395 nm was placed in front of the aperture in order to avoid second order effects. Wavelength-resolved extinction measurements on laser-irradiated soot particles were performed in the 400 to 800 nm spectral region. For these measurements, a low resolution grating (150 grooves/mm) was used, resulting in 0.28 nm spectral resolution.

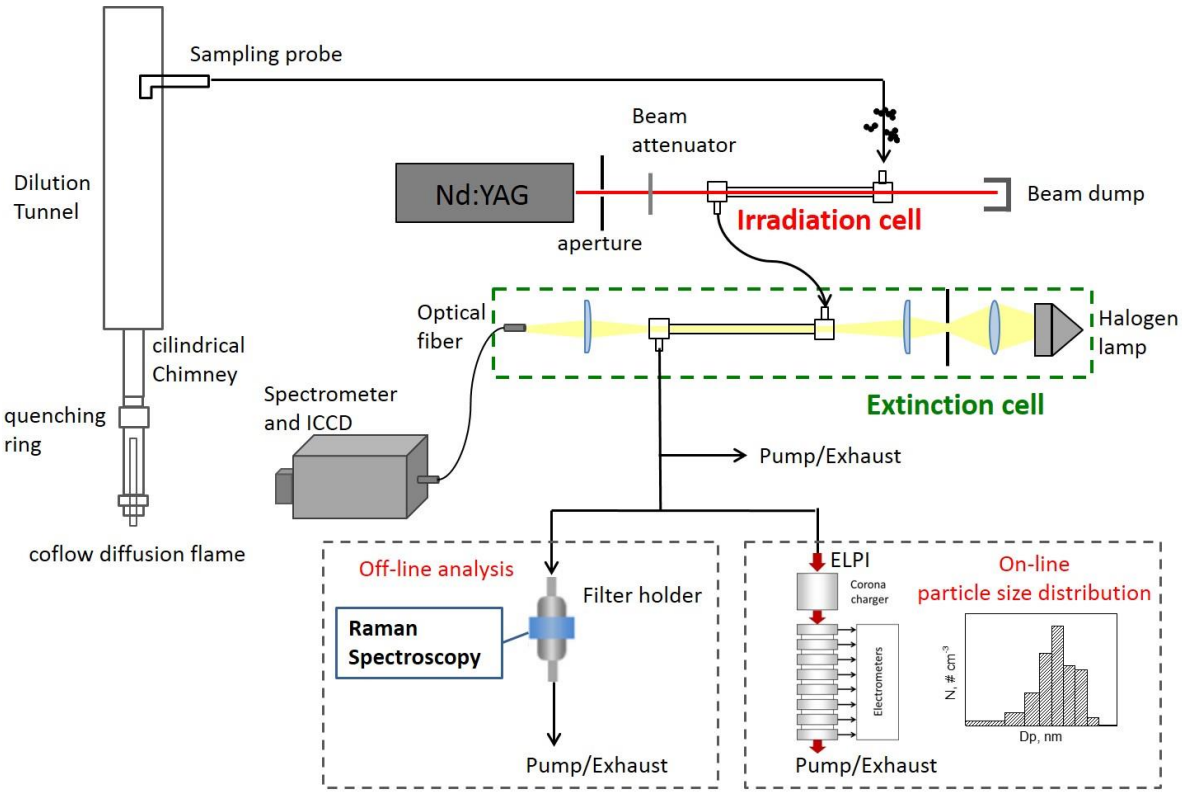

Figure 1. Schematic of the experimental set-up.

At the end of the extinction line the particles were either collected on a glass fiber filter (Watmann, ∅ = 47 mm) for Raman spectroscopy analysis or pumped into an electrical low pressure impactor (ELPI, Dekati) for on-line particle size distributions measurements. A sketch of the experimental apparatus is reported in Figure 1.

https://doi.org/10.1016/j.expthermflusci.2020.110064

The filters covered by soot particles were directly positioned under the Raman microscope (Horiba XploRA) equipped with a 100× objective (NA0.9, Olympus) without further manipulation. The laser source was a Nd:YAG laser (λ = 532 nm, 12 mW maximum laser power at the sample). Spectra were obtained with a laser beam power of 1%, and an accumulation-exposure time of five cycles of 20 s each. All the Raman spectra were background subtracted and normalized to their maximum value.

3. Results and discussion

The spectral dependence of the optical properties of non-irradiated and laser-irradiated particles was investigated by performing extinction measurements. In particular, according to the Beer-Lambert law**:**

$$\tau_\lambda = \frac{I_{\lambda,T}}{I_{\lambda,0}} = \exp\left(-\int_0^L K_{ext,\lambda}\, dx\right) \quad (1)$$

where $I_{\lambda,T}$ is the transmitted light, $I_{\lambda,0}$ is the incident light, K_{ext} is the extinction coefficient of the dispensed particles and x is the spatial location along the path. If the medium is uniform along the line-of sight, Eq. 1 simplifies to:

$$-\ln \tau_\lambda (y) = K_{ext,\lambda}\, L \quad (2)$$

where L is the optical path length.

Particles were irradiated using different laser fluences, from 0 to 0.7 J/cm^2. The extinction data were collected after the laser-irradiated particles had cooled down to ambient temperature.

Figure 2 shows the spectral behaviour of the extinction coefficient of non-irradiated and irradiated soot nanoparticles for both ethylene (Fig.2a) and methane (Fig.2b) flames. The uncertainty associated with the transmissivity measurements is about 3 %.

https://doi.org/10.1016/j.expthermflusci.2020.110064

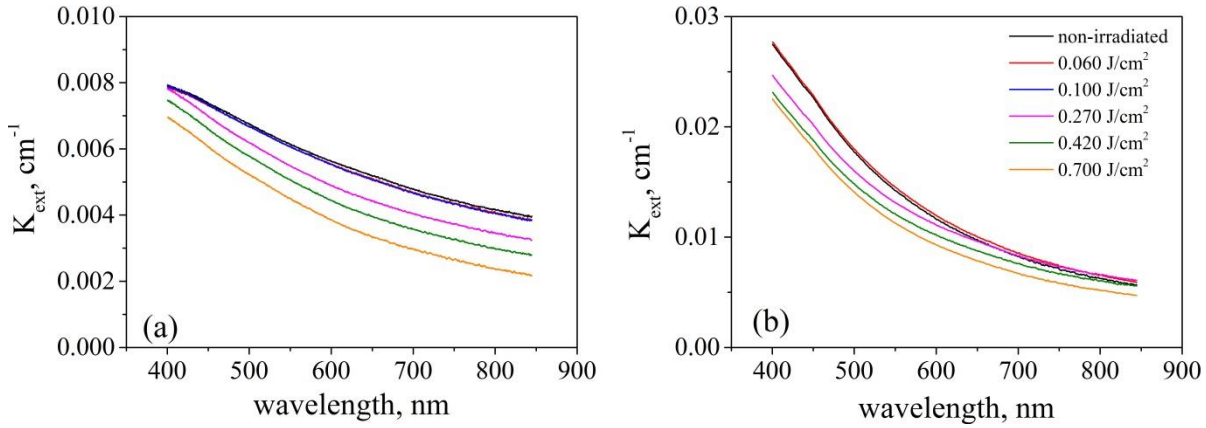

Figure 2. Extinction coefficient of cold and laser-irradiated particles at different laser fluences: (a) ethylene, (b) methane.

A significant variation in the extinction coefficient of laser-irradiated soot particles compared to the pristine ones can be observed in both cases. In particular, no variation of K_{ext} is observed for laser fluences up to 0.1 J/cm^2 for both ethylene and methane soot. Then, the extinction coefficient decreases at increasing laser fluence. Such reduction is partly due to sublimation of soot particles at very high laser energy density. In fact, it has been demonstrated in a previous work that independently from the nature of the investigate soot particles, for fluences higher than approximately 0.3 J/cm^2 soot particles reach the sublimation temperature of about 4000K [9]. However, a different spectral behaviour of K_{ext} is also observed. For shorter wavelengths a steeper slope of the extinction coefficient is detected for the irradiated nanoparticles, especially for ethylene.

It is noteworthy that the extinction coefficient is made by two contributions, namely absorption and scattering. For the type of soot generated in our case, it is reasonable to assume that aggregate size is on the order of 100 nm and consequently single scattering albedo (defined as scattering coefficient over extinction coefficient) is not negligible. To quantify this effect, scattering measurements were performed at 470 nm, using a CW Ar-Kr laser, for ethylene soot, which exhibits a stronger variation than methane in the optical properties of irradiated particles. Being the shorter wavelength more scattered (scattering signal $\propto \lambda^{-4}$), scattering contribution to extinction is more significant at these wavelengths. The light scattered by non-irradiated and irradiated soot particles was collected at 45° respect to the incident laser beam. To this purpose a new extinction cell was implemented, allowing the detection of the light at such angle. Extinction measurements were performed simultaneously to scattering in order to obtain the single scattering albedo at 470 nm. Figure 3 shows the single scattering albedo behavior with laser fluence, together with the related uncertainty, which is about 6%.

https://doi.org/10.1016/j.expthermflusci.2020.110064

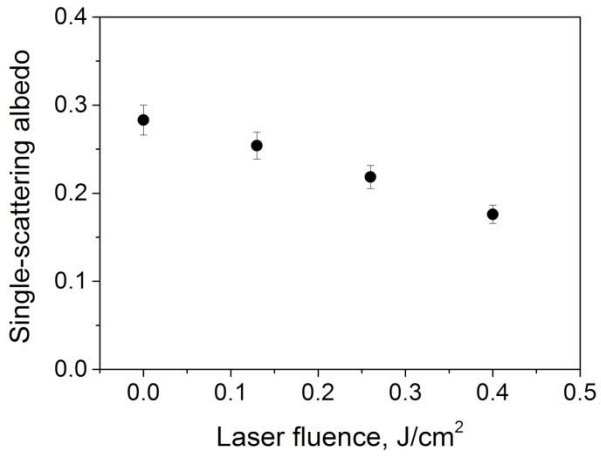

Figure 3. Single-scattering albedo at 470 nm versus laser fluence.

Non-irradiated particles exhibit single-scattering albedo of 0.28, which is in good agreement with the data reported in literature for mature soot [8, 19-20]. For irradiated particles a reduction of the single-scattering albedo with laser fluence was detected, as also observed by Michelsen and co-workers at 532 and 1064 nm [8]. Therefore, it is reasonable to assume that the enhancement in the slope of the extinction coefficient at shorter wavelengths is due to a real change in the absorption properties and not caused by an increase of the scattering contribution.

To better appreciate the difference in the extinction coefficient curves with laser fluences, the K_{ext} spectra have been fitted by a power-law function. In fact, in early pioneering studies it was proved that the extinction coefficient follows the empirical relation $\boldsymbol{K_{ext} = c\lambda^{-\alpha}}$ where c is a function of the particle concentration and α is the dispersion exponent [21]. The values of the dispersion coefficient derived by fitting the curves in Fig. 2 are reported in Table 2. The uncertainty associated to the reported α values is approximately 10%.

Table 2. Dispersion coefficient.

	α - Ethylene	α - Methane
Non-irradiated	1.02	2.22
0.060 J/cm^2	1.04	2.16
0.100 J/cm^2	1.04	2.14
0.270 J/cm^2	1.23	1.92
0.420 J/cm^2	1.38	1.95
0.700 J/cm^2	1.63	2.16

https://doi.org/10.1016/j.expthermflusci.2020.110064

For the ethylene soot, an increase in the α value is observed with laser irradiation. The α value for methane soot is shown to be rather constant with laser irradiation. Moreover, the α coefficients obtained for methane are higher than those from ethylene. Previous works showed that, for mature soot, with small spectral dependency of refractive index, the dispersion exponent is α~1. By contrast, larger values of α have been reported for incipient soot as due to a different structural/chemical composition of the particles and a larger H/C ratio [22]. Therefore, the increase of α, observed for the irradiated soot by increasing the laser fluence, could be indicative of a change in the chemical/structural composition of the particles although it may also indicate that the morphology and size of the particles, more than the composition, is playing a role in the change of the extinction spectra [23-24].

Laser-heating of soot particles is known to produce changes in their inner structure as detected by TEM [11-12] and HRTEM analysis [10, 25]. Very recently, Vander Wal and co-authors [18] examined a variety of soots annealed by single pulse laser irradiation, among them soot produced in ethylene co-flow diffusion flames. The authors showed that the diversity of nanostructures, observed across the various carbons upon pulsed laser irradiation, is ascribed to variable initial physical nanostructure along with the chemistry of formation [18]. It is reasonable to expect that a change in the inner structure would also affect the optical properties of these particles, in particular their refractive index.

Another method for the analysis of the absorption characteristics of a carbonaceous material is represented by the analysis of the optical band gap (OBG), i.e., the energy threshold for photon absorption. The optical band gap can be experimentally evaluated from the UV-visible absorption spectrum using the Tauc equation [26]:

$$\sqrt{\boldsymbol{K_{ext}E}} = \boldsymbol{B}\left(\boldsymbol{E} - \boldsymbol{E_g}\right) \tag{3}$$

where E is the energy of the incident photon, B is a constant, and E_g is the Tauc optical gap. Thus, by plotting $\sqrt{\boldsymbol{K_{ext}E}}$ as function of E and extrapolating the linear slope to zero absorption, the optical band gap can be estimated. Figure 4 shows the variation of the OBG with laser fluence for both ethylene and methane soot.

https://doi.org/10.1016/j.expthermflusci.2020.110064

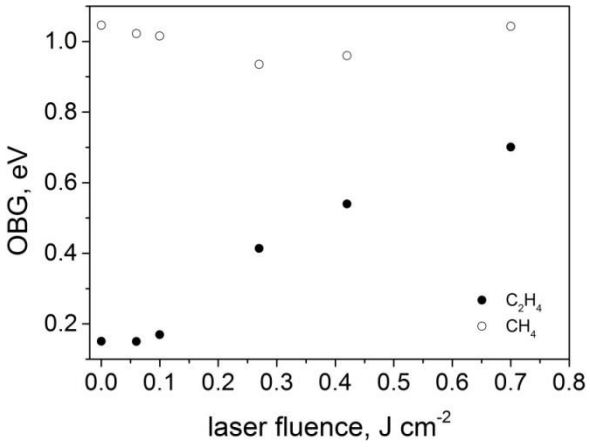

Figure 4. Optical band gap versus laser fluence.

For ethylene, the OBG is initially very low and increases as particles are irradiated suggesting a decrease in the sp^2 content of the material and therefore a sort of "amorphization" of the particles. On the other hand, the OBG for methane soot, which is initially of the order of 1 eV, remains approximately constant in the range of fluences investigated. These results are consistent with the results from two color LII measurements reported in previous works [9, 11]. However, they are in contrast with the OBG data of Singh et al. [27]. These authors analyzed the effect of laser radiation on two commercially available carbon blacks which could be chemically and structurally very different from soot. The optical band gap of the irradiated particles was found to be lower than the OBG of the non-irradiated ones suggesting a larger number of aromatic rings in the aggregate and a greater π conjugation, thus a graphitic-like structure [27].

In order to understand if changes in soot nanostructure are responsible for the observed changes in the optical properties of the irradiated soot particles, a Raman spectroscopy analysis of the irradiated and non-irradiated soot particles collected on quartz filter was performed. Figure 5 reports the first-order Raman spectra of soot not exposed to the laser radiation and exposed to laser light at different fluences for both flames.

https://doi.org/10.1016/j.expthermflusci.2020.110064

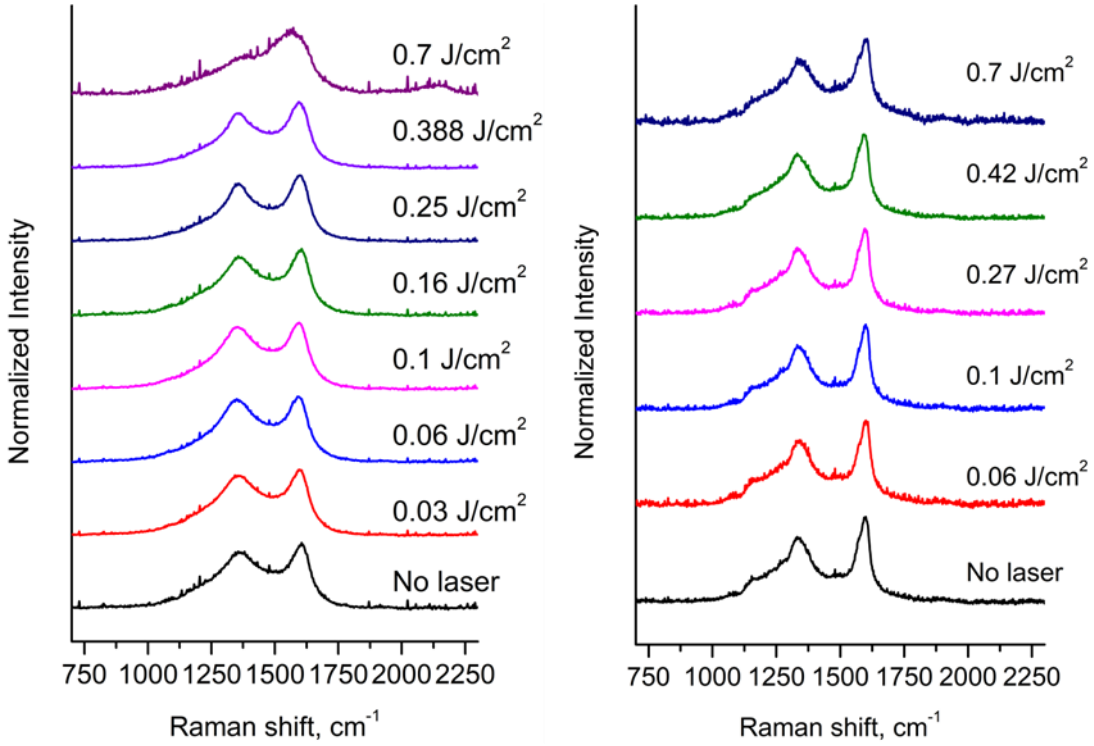

Figure 5. Raman spectra of non-irradiated and radiated soot particles: (a) soot from ethylene flame; (b) soot from methane flame. Each spectrum has been background subtracted, normalized to the maximum, and the curves are vertically translated for a clarity.

All the Raman spectra present the two Raman bands characteristic of carbon-based materials: the D band at a Raman shift of about ~1350 cm^{-1} and the G band at ~1600 cm^{-1}. The latter is produced by phonon modes with E_{2g} symmetry and is Raman active for every hybridized sp^2 carbon. The D band is due to phonons that are produced by the ring breathing mode with A_{1g} symmetry from sp^2 carbon rings. This band, however, requires edges or defects to be activated so that it appears in nano-crystalline graphite, due to edge effects, or in defected and amorphous carbon [28].

The relative intensity, the widths and the position of these two bands give indications on the carbon structure of the sample [28]. The main difference in the spectra of samples subjected to different laser irradiations consists in the relative intensity of the two bands. The trends of $I(D)/I(G)$ versus the laser fluence are reported in Fig. 6.

https://doi.org/10.1016/j.expthermflusci.2020.110064

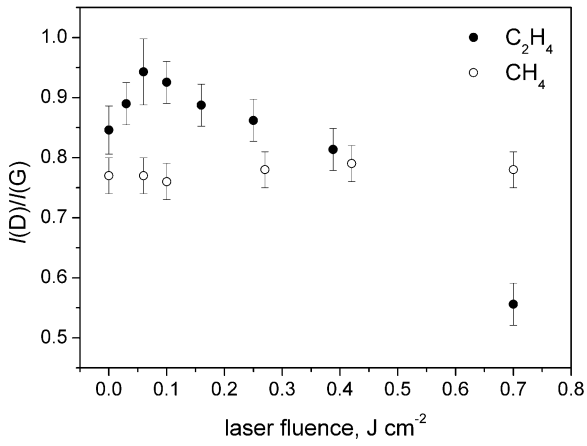

Figure 6. *I*(D)/*I*(G) as function of laser fluence.

Soot extracted from methane and ethylene flames exhibit different trends as function of the laser fluence. Soot from the ethylene flame shows a non-monotonic trend: increases up to the fluence of 0.06 J/cm^2, where the band gap remains very low, and then starts decreasing reaching the value of 0.56 for the 0.7 J/cm^2 sample, whose spectrum significantly differs from all the others. Indeed, the G line sensibly broadens towards lower wavenumber shifting the maximum down to 1570 cm^{-1}. A Raman G band positioned at 1570 cm^{-1} has been found to be representative of onion like carbon [29], the appearance of this feature in our sample may thus indicate that spherical sp^2 shell are formed by such strong laser irradiation. It is worth noticing that onion-like structures produced by multiple laser-shot irradiation of soot generated in the same ethylene flame were visualized in a previous work by TEM [9]. At fluences below 0.7 J/cm^2, the laser irradiation probably produces an increase of sp^2 region although the formation of the shell is not complete. In this case, the Raman spectrum is more similar to that of a disordered, polycrystalline carbon, since the correlation length for the phonons is determined by the size of the ordered sp^2 region in partial shells and not by a fully developed shell. The Raman spectrum of the 0.7 J/cm^2 sample also presents an additional peak at 2150 cm^{-1}, which is indicative of polyacetylene-like functionalities that are presumably formed as a consequence of the laser-induced partial fragmentation/vaporization of soot particles [30]. Different is the case of soot from methane flame, where no significant changes have been observed which are in perfect agreement with the extinction measurements and the OBG trend.

Particles nanostructure is not the only parameter affecting particle optical properties. Potential changes in soot morphology may play an important role as well. Among them, aggregation is of major concern. Liu et al. [23] have found that absorption cross section is sensibly dependent on particle aggregation. Both the aggregate size and the primary particle

https://doi.org/10.1016/j.expthermflusci.2020.110064

size can either enhance or reduce the absorption cross section through electric field coupling and shielding effects.

Michelsen et al. [8] performed LII and transmittance measurements at 532 and 1064 nm in an ethylene diffusion flame and observed an increase in the absorption cross section with increasing laser fluences while the scattering cross section decreases. The increase in the absorption cross section was attributed to either an increase in the primary particles size with temperature-induced swelling or temperature dependent changes of the optical properties. The trend of the scattering cross section was attributed to a change in the optical properties of the particle or to a change in the morphology of the particle with temperature.

Filippov et al. [31] observed that the irradiation of spark generated graphite agglomerates causes a reduction of the size and a decrease of the distribution width by increasing laser fluence. This fact was ascribed to the partial disintegration of the agglomerates caused by the coulombic repulsion forces due to the thermoelectron emission induced by laser heating.

To investigate the effect of laser irradiation on particle size, we have measured the particle size distributions of non-irradiated and irradiated nanoparticles using an electrical impactor and the results are reported in Fig. 7 (black bars for ethylene and red bars for methane). The particle number is normalized to the total particle number in each condition. The size distribution of non-irradiated particles has mean aerodynamic diameter of about 200 and 150 nm for ethylene and methane, respectively. For ethylene soot, all the distributions of laser-irradiated particles show a significant reduction in the mean aerodynamic diameter and a strong increase in number density of very small particles. This trend suggests that most of the particles sampled from the quenched flame consist of aggregates. Increasing the laser fluence, the number of these aggregates decreases while small particles are formed. This can be due to a significant fragmentation of the aggregates into primary particles, as advanced by Filippov et al. [31], and/or by their vaporization followed by nucleation of new particles, as previously reported by Michelsen et al. [12].

For methane soot, no significant difference in the particle size distribution is observed for fluences up to 0.1 J/cm^2. For higher fluences, a behaviour similar to ethylene soot is detected.

https://doi.org/10.1016/j.expthermflusci.2020.110064

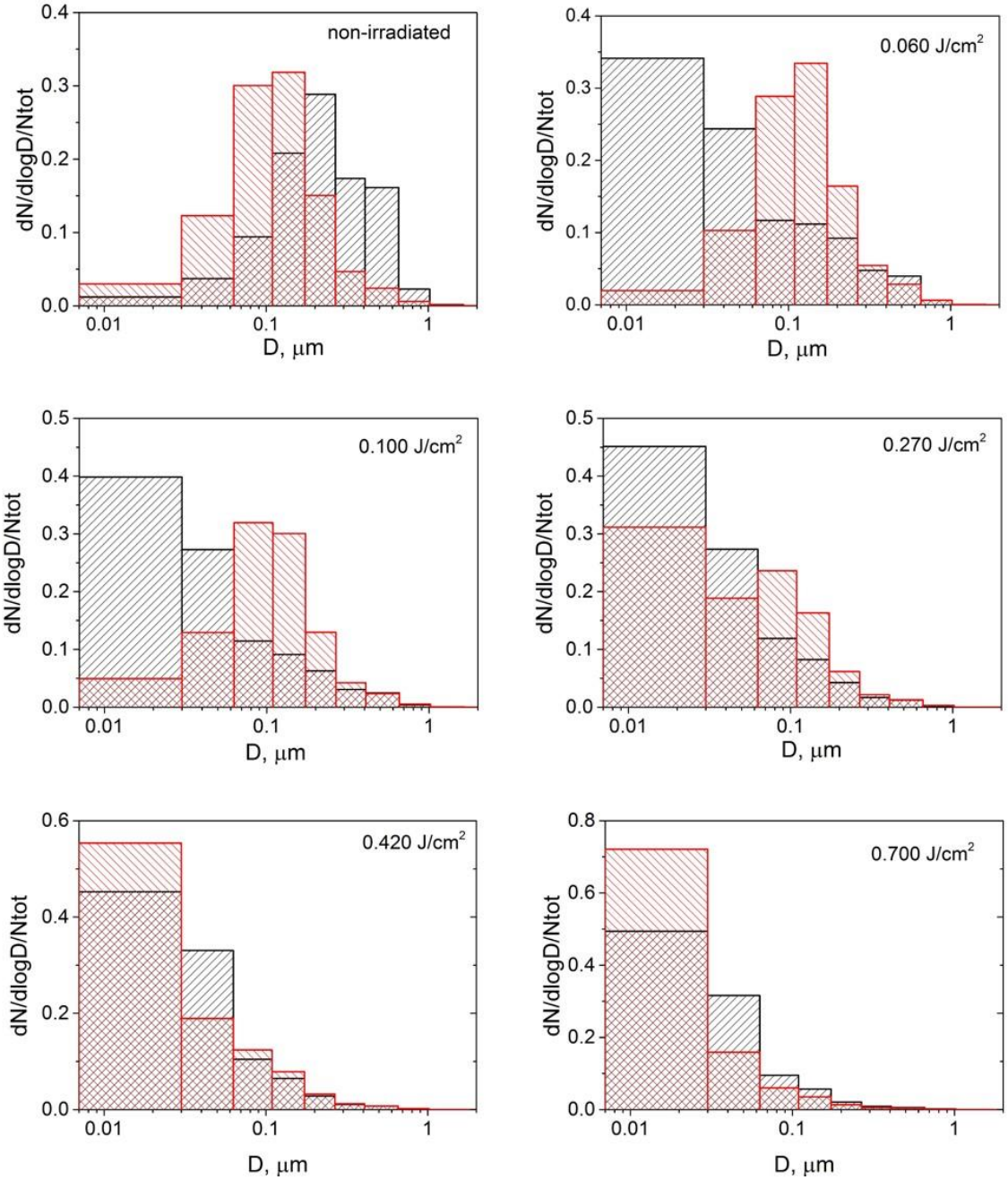

Figure 7. Particle size distribution of non-irradiated and laser-irradiated particles. Ethylene: black bar, methane: red bars

This result highlights the different nature of soot particles generated by ethylene or methane. Particles fragmentation can be due either to a thermal or an oxidative process. In our experiment, we definitively have excess of oxygen being the exhaust of the quenched coflow diffusion flames diluted with air. To discriminate between the two processes, a test with pure Nitrogen as dilution gas has been performed. The aerodynamic size distributions of non-irradiated and laser-irradiated particles obtained after Nitrogen dilution show the exact same

https://doi.org/10.1016/j.expthermflusci.2020.110064

behaviour of the particles diluted in air. Therefore, we can exclude that, in our experimental conditions, fragmentation results from particle oxidation. Regardless of the mechanism, the observed fragmentation could be partially responsible for the variation in the optical properties. Nevertheless, the results in Fig. 7, together with the Raman analysis of the irradiated soot particles, seem to indicate that changes in soot structure after laser irradiation is the major effect accounting for the observed variation in optical properties.

4. Conclusion

Soot extracted from two laminar diffusion flames respectively fueled by ethylene and methane was analyzed in term of physicochemical properties under a variety of laser heating conditions. In particular the analysis was focused on the optical properties, nanostructure and size/morphology of those particles.

Wavelength-resolved extinction measurements highlighted a significant variation in the optical properties of laser-irradiated particles. Especially for ethylene soot, a different spectral behavior of K_{ext} is observed at fluences higher than approximately 0.27 J/cm^2. Exceptionally, a stronger slope of K_{ext} at short wavelength is noticed. Such behavior is emphasized by the related dispersion coefficient, which increases increasing laser fluence. For methane soot, the dispersion coefficient is rather constant with fluence but is higher than the value for ethylene, indicating a different chemical/structural composition between the two types of soot particles. In fact, also the nanostructure of irradiated ethylene and methane soot particles behaves differently. While the nanostructure of methane soot is not significantly affected by laser irradiation, a strong modification is observed for ethylene soot. In particular, at very high laser fluence, laser irradiation seems to promote the formation of onion-like carbon structure. Particle size distribution measurements show that aggregates undergo a strong fragmentation. It is reasonable to assume that smaller aggregates as well as new small particles with different nanostructure would have different optical properties.

In summary, our results indicate that soot nanostructure and optical properties are strongly dependent on the fluence intensity when irradiated by a laser source. This is significant for ethylene soot, while for methane soot the degree of variation of such properties is less pronounced, at least in the investigated heating conditions.

It is important to stress that the variation of the optical properties under laser irradiation has a strong impact on the application and interpretation of laser-based diagnostics, especially the laser-induced incandescence technique. Finally, since the effect of laser irradiation strongly

dependents on the fuel used for generating the soot particles, laser irradiation may be also used as soot source apportionment.

Acknowledgment

The authors acknowledge the financial support from the PRIN project 2017PJ5XXX: "Modeling and Analysis of carbon nanoparticles for innovative applications Generated dIrectly and Collected DUring combuSTion (MAGIC DUST)".

References

[1] C.A. Pope, D.W. Dockery, Health effects of fine particulate air pollution: Lines that connect, J. Air Waste Manage. Assoc. 56 (2006) 709-742.

[2] T.C. Bond, S.J. Doherty, D.W. Faethy, P.M. Forster, T. Berntsen, B.J. DeAngelo, et al., Bounding the role of black carbon in the climate system: A scientific assessment, J. Geophys. Res. 11(2013) 5380-5552.

[3] H. Moosmüller, R. Chakrabarty, W. Arnott, Aerosol light absorption and its measurement: A review, J. Quant. Spectrosc. Radiat. Transfer 110 (2009) 844-878.

[4] A. D'Alessio, A. D'Anna, G. Gambi, P. Minutolo, The spectroscopic characterization of UV absorbing nanoparticles in fuel rich soot forming flames, J. Aerosol Sci. 29 (4) (1998) 397- 409.

[5] H.A. Michelsen, C. Schulz, G.J. Smallwood, S. Will, Laser-induced incandescence: Particulate diagnostics for combustion, atmospheric, and industrial applications, Prog. Energy Combust. Sci., 51(2015) 2-48.

[6] F. Migliorini, S. De Iuliis, S. Maffi, G. Zizak, Environmental application of laser-induced incandescence, Appl. Phys. B: Lasers Opt. 112 (2013) 433-440.

[7] L.A. Melton, Soot diagnostics based on laser heating, Appl. Opt. 23 (1984) 2201-2208.

[8] H.A. Michelsen, P.E. Schrader, F. Goulay, Wavelength and temperature dependences of the absorption and scattering cross sections of soot, Carbon 48 (2010) 2175-2191.

[9] F. Migliorini, S. De Iuliis, S. Maffi, G. Zizak, Saturation curves ot two-color laser-induced incandescence measurements for the investigation of soot optical properties, Appl. Phys. B: Lasers Opt. 120 (2015) 417-427.

[10] R.L. Vander Wal, M.Y. Choi, Pulsed laser heating of soot:morphological changes, Carbon 37 (1999) 231-239.

https://doi.org/10.1016/j.expthermflusci.2020.110064

[11] S. De Iuliis, F. Cignoli, S. Maffi, G. Zizak, Influence of the cumulative effects of multiple laser pulses on laser-induced incandescence signals from soot, Appl. Phys. B: Lasers Opt. 104 (2011) 321-330.

[12] H.A. Michelsen, A.V. Tivanski, M.K. Gilles, L.H. van Poppel, M.A. Dansson, P.R. Buseck, Particle formation from pulsed laser irradiation of soot aggregates studied with a scanning mobility particle sizer, a transmission electron microscope, and a scanning transmission x-ray microscope, Appl. Opt. 49 (2007) 959-977.

[13] R.L. Vander Wal, T.M. Ticich, A.B. Stephens, A., Optical and microscopy investigations of soot structure alterations by laser-induced incandescence, Appl. Phys. B: Lasers Opt. 67 (1998) 115-123.

[14] P.O. Witze, S. Hochbreg, D. Kayes, H.A. Michelsen, C.R. Shaddix, Time-resolved laser-induced incandescence and laser elastic-scattering measurements in a propane diffusion flame, Appl. Opt. 40 (2001) 2443-2452.

[15] N.-E. Olofsson, J. Johnsson, H. Bladh, P.-E. Bengtsson, Soot sublimation studies in a premixed flat flame using laser-induced incandescence (LII) and elastic light scattering (ELS), Appl. Phys. B: Lasers Opt. 112 (2013) 333-342.

[16] M. Saffaripour, K.-P. Geigle, D.R. Snelling, G.J. Smallwood, K.A. Thomson, Influence of rapid laser heating on the optical properties of in-flame soot, Appl. Phys. B: Lasers Opt. 119 (2015) 621-642.

[17] K.A. Thomson, K.-P. Geigle, M. Köhler, G.J. Smallwood, D.R. Snelling, Optical properties of pulsed laser heated soot, Appl. Phys. B: Lasers Opt. 104 (2011) 307-319.

[18] M. Singh, C.K. Gaddam, J.P. Abrahamson, R.L. Vander Wal, Soot differentiation by laser derivatization, Aerosol Sci. Technol. 53 (2) (2019) 207-229.

[19] J. Zhu, M.J. Choi, G.W. Mulholland, L.A. Gritzo, Soot scattering measurements in the visible and near-infrared spectrum, Proc. Combust. Inst. 28 (2000) 439-446.

[20] J. Yon, R. Lemaire, E. Thersen, P. Desgroux, A. Coppalle, K.F. Ren, Examination of wavelength dependent soot optical properties of diesel and diesel/rapeseed methyl ester mixture by extinction spectra analysis and LII measurements, Appl. Phys. B: Lasers Opt. 104 (2011) 253-271.

[21] R.C. Millikan, Optical properties of soot, J. Opt. Soc. Am. 51 (1961) 698-699.

[22] P. Minutolo, G. Gambi, A. D'Alessio, The optical band gap model in the interpretation of the UV-visible absorption spectra of rich premixed flames, Proc. Comb. Inst. 26 (1996) 951-957.

https://doi.org/10.1016/j.expthermflusci.2020.110064

[23] F. Liu, G.J. Smallwood, Effect of aggregation on the absorption cross-section of fractal soot aggregates and its impact on LII modelling, J. Quant. Spectrosc. Radiat. Transfer 111 (2010) 302-308.

[24] C. Liu, A. Singh, C. Saggese, Q. Tang, D. Chen, K. Wan, M. Vinciguerra, M. Commodo, G. De Falco, P. Minutolo, A. D'Anna, H. Wang, Flame-Formed Carbon Nanoparticles Exhibit Quantum dot behaviors, Proc. Natl. Acad. Sci. U.S.A. 116 (26) (2019) 12692-12697.

[25] B. Apicella, P. Pré, J.N. Rouzaud, J. Abrahamson, R.L. Vander Wal, A. Ciajolo, et al., Laser-induced structural modifications of differently aged soot investigated by HRTEM, Combust. Flame 204 (2019) 13-22.

[26] J. Tauc, R. Grigorovici, A. Vancu, Optical Properties and Electronic Structure of Amorphous Germanium, Phys. Stat. Sol. 15 (1966) 627-367.

[27] M. Singh, J.P. Abrahamson, R.L. Vander Wal, Informing TiRe-LII assumption for soot nanostructure and optical properties for estimation of soot primary diameter, Appl. Phys. B: Lasers Opt. 124 (2018) 130.

[28] A.C. Ferrari, D.M. Basko, Raman spectroscopy as a versatile tool for studying the properties of graphene, Nature Nanotech. 2013, 8 235–246.

[29] D. Roy, M. Chhowalla, H. Wang, N. Sano, I. Alexandrou, T.W. Clyne, G.A.J. Amaratunga, Characterisation of carbon nano-onions using Raman spectroscopy, Chem. Phys. Lett. 373 (2003) 52–56.

[30] F. Innocenti, A. Milani, C. Castiglioni, Can Raman spectroscopy detect cumulenic structures of linear carbon chains?, J. Raman Spectrosc. 2010, 41, 226–236.

[31] A.V. Filippov, M.W. Markus, P. Roth, In-situ characterization of ultrafine particles by laser-induced incandescence: sizing and particle structure determination, J Aerosol Sci. 30 (1) (1999) 71-87.